Biophysical controls on seasonal changes in the structure, growth, and grazing of the size-fractioned phytoplankton community in the northern South China Sea

5 Yuan Dong[1,2], Qian P. Li[1,2,3]*, Zhengchao Wu[1,2], Yiping Shuai[1,3], Zijia Liu[1,3], Zaiming Ge[1,3], Weiwen Zhou[1,3], and Yinchao Chen[1,3]

[1]State key Laboratory of Tropical Oceanography, South China Sea Institute of Oceanology, Chinese Academy of Sciences, Guangzhou, China

10 [2]Southern Marine Science and Engineering Guangdong Laboratory (Guangzhou), Guangzhou, China

[3]College of Marine Science, University of the Chinese Academy of Sciences, Beijing, China

*Correspondence to: Qian P. Li (qianli@scsio.ac.cn)

Abstract. The size-fractionated phytoplankton growth and microzooplankton grazing are crucial for the temporal
15 change of community size-structure, regulating not only trophic transfer but also the carbon cycle of the ocean. However, the size-dependent growth and grazing dynamics on monthly or an annual basis are less addressed in the coastal ocean. In this paper, the seasonal responses of the size-fractionated phytoplankton growth and grazing to environmental change were examined over one year at a coastal site of the northern South China Sea. We found a nanophytoplankton dominated community with strong seasonal variations of all size classes. Phytoplankton community growth rate was positively
20 correlated to nutrients with community grazing rate correlating to the total chlorophyll-*a* at the station, reflecting a combined bottom-up and top-down effect on phytoplankton population dynamics. Further analyses suggested that the specific growth rate of microphytoplankton was significantly influenced by phosphate with that of nanophytoplankton by light, although picophytoplankton growth was controlled by both nitrate and temperature. In addition, the specific grazing rate of nanophytoplankton was well correlated to phytoplankton standing stock, while those of micro- and pico-compartments were
25 negatively influenced by ciliate abundance and salinity. Finally, a lower grazing impact for micro-cells (38%) than nano- and pico-cells (72% and 60%, respectively) may support size-selective grazing of microzooplankton on small cells at this eutrophic system.

1. Introduction

Plankton are the basic components of the aquatic food web. Phytoplankton growth can be influenced by nutrient availability (such as nitrogen, phosphorus, silica, or iron) via the bottom-up effect and/or zooplankton grazing via the top-down effect (Strom et al., 2007). Grazing of bacterioplankton by microzooplankton (such as nanoflagellates and ciliates) has been well-known in aquatic environments (Ichinotsuka et al., 2006; Unrein et al., 2007; Schmoker et al., 2013). Microzooplankton are generally the dominant herbivores in the marine ecosystem (Calbet and Landry, 2004), regulating not only primary productivity but also carbon export via vertical migration/pellet sinking and nutrient recycling by mixotrophy (Steinberg and Landry, 2017). Spatial changes of phytoplankton growth and microzooplankton grazing have been well appreciated in the coastal ecosystems due to rapidly varying environmental conditions such as temperature, nutrients, and light (e.g. Landry et al., 2009; Li et al., 2012; Dong et al., 2018). In contrast, temporal variabilities in rate processes over an annual cycle or monthly are often less addressed, not to mention the relevant controlling mechanisms (Chen et al., 2009; Anderson and Harvey, 2019). This aspect of temporal dynamics, however, may be essential for understanding the long-term change of biological productivity, community structure, and ecosystem functions in the coastal oceans.

The coastal regions of the northern South China Sea (NSCS) are subject to strong influences by complex physical processes, such as wind-induced mixing, coastal upwelling, river discharge, and atmospheric deposition. Seasonal variation of primary productivity over the NSCS shelf could be related to hydrographic dynamics driven by varying monsoon winds with a stronger turbulent mixing during the winter (e.g. Liu et al., 2002). Furthermore, nutrient concentration and stoichiometry of the surface waters could be influenced by the interplay between river discharge (a high N/P ratio) and coastal upwelling (a low N/P ratio) over the inner shelf of the NSCS (Gan et al., 2010), leading to intense phytoplankton blooms during the summer. In addition, the river plume would affect the size-structure of the phytoplankton community with large-sized phytoplankton such as diatoms well promoted at the frontal zone (Li et al., 2018). Finally, atmospheric depositions of nutrients and toxic metals could also largely affect coastal phytoplankton growth and the community compositions of the nearshore waters in the NSCS (Zhou et al., 2021).

The Pearl River Estuary (PRE), with an area of about 4.5×10^5 km^2, is one of the largest river systems in the northern South China Sea (NSCS). Wanshan archipelago, located at the mouth of the PRE, is the primary channel for the Pearl River waters entering the shelf-sea. Therefore, the surrounding waters near Wanshan often showed a rapid change of salinity and nutrients due to the interplay between the estuarine freshwater and the adjacent coastal seawater. Similar to many other estuarine-coastal ecosystems around the world (Cloern et al., 2014), there is high production at the estuary mouth near the Wanshan region but low production in the turbidity maximum zone within the estuary. Phytoplankton in the coastal waters near Wanshan is dominated by fast-growing diatoms in response to strong eutrophication (e.g. Li et al., 2013). The dominant diatom species here are *Skeletonema costatum* in the summer and *Eucampia zoodiacus* in the winter, which are intensively grazed by ciliates and dinoflagellates, as well as copepods (Chen et al., 2015). Further studies suggest that phytoplankton

growth here is influenced by nutrient limitation (Li et al., 2018), size-selective microzooplankton grazing (Dong et al., 2018), and the deterrent effect of phytoplankton-derived oxylipins on zooplankton grazers (Wu and Li, 2016). Meanwhile, it remains less studied about the seasonal patterns of phytoplankton productivity and the grazing activity of microzooplankton in the coastal waters outside the highly euphotic estuary.

In this study, we focus on a coastal time-series station near the Wanshan to explore the monthly change of the plankton ecosystem from June 2018 to June 2019. We have performed comprehensive measurements of the plankton community, including the chlorophyll-a size-fractionation, the picophytoplankton composition by flow cytometry, the nano- and microplankton abundances by FlowCAM, and the size-fractionated growth and grazing rates by dilution experiments. Based on these data, we investigate the seasonal variabilities of phytoplankton size structure and size-fractionated growth rates. We explore the relationships of these variabilities with changing environmental conditions such as temperature, light, and nutrients. We also examine the monthly variability of microzooplankton and their size-dependent feeding. Seasonal changes in growth and grazing rates, as well as size-selective prey preference at a coastal site such as Wanshan could be crucial for understanding the temporal dynamics of food-web structure, carbon export, and nutrient recycling in the coastal ocean (e.g. Steinberg and Landry, 2017). Moreover, our results here may be of great value for modeling the size-structured planktonic ecosystem and associated element cycles as temporal variabilities of these processes are often not well represented in current biogeochemical models (e.g. Li et al., 2011; Sailley et al., 2015).

2. Materials and Methods

2.1 Description of the field study and measurement of environmental parameters

We also conducted monthly hydrographic and biogeochemical monitoring, as well as phytoplankton chlorophyll-*a* size-fractionation and size-specific dilution experiments at the Wanshan station (Fig. 1) from June 2018 to June 2019. This station (21.9°N, 113.8°E) is located near the Wanshan Island of the NSCS with a water depth of ~28 m (see Fig. 1). Water temperature and salinity were measured using a pre-calibrated YSI multi-probe sensor. Surface waters at ~2 m (about 100 L) were directly collected with an acid-cleaned polycarbonate bucket. After removing the larger grazers (>200 μm) using a 200-μm mesh, water samples were gently transferred to polycarbonate bags in a temperature-controlled cooler in the dark.

The sample for inorganic nutrients, including nitrate (NO_3^-), phosphate (PO_4^{3-}), and silicate (SiO_3^{2-}), was pre-filtered through a GF/F filter and frozen immediately at −20℃ in a freezer. Samples were thawed at room temperature and measured by a Seal AA3 auto-analyzer (Bran-Luebbe, GmbH) using the classic colorimetric methods (Hansen and Koroleff, 1999). The monthly solar radiation data was acquired from a nearby weather station in Hong Kong City (https://www.hko.gov.hk).

90 There were three major subbranches of the Pearl River system (West, North, and East rivers), flowing into the shelf-sea through eight different outlets. The total flow rate to the Wanshan station was estimated by the sum of three major entrances at Humen, Modaomen, and Jiaomen (Guangdong Hydrographic Bureau, http://swj.gd.gov.cn/zwgk_tjxx/index.html).

To show the typical difference in the hydrographic characters of the coastal NSCS between winter and summer, sectional data of two cruises crossing the Wanshan station during December 2006 and June 2019 were used (Fig. S1). The
95 vertical transects covered the major river-influenced area from the estuary to the inner shelf of the NSCS. The profiles of seawater temperature, salinity, and pressure were continuously measured using a Sea-Bird model SBE9/11 conductivity-temperature-depth (CTD) sensor.

2.2 Phytoplankton and zooplankton measurements

100 After returning to the laboratory (<1 hour), the Chl-*a* size-fractionation for micro- (20-200 μm), nano-(2-20 μm), and pico-phytoplankton (<2 μm) (Dong et al., 2018) were performed immediately. Duplicated seawater samples (1~2 L) were processed through a sequence of filtration steps under a low vacuum (<50 kPa), including a 20-μm pore size Nylon membrane filter, a 2-μm pore size polycarbonate filter, and a GF/F filter. Total Chl-*a* was calculated as the sum of the Chl-*a* concentrations of the three different size classes. The filters were extracted in 90% acetone for at least 18 h in the dark at
105 −20°C. After centrifuging at 4000 rpm for 10 min, the Chl-*a* concentration was determined by a Turner Designs Model 10 Fluorometer (Parsons et al., 1984).

For picoplankton, a volume of 2-mL seawater sample was pre-filtered by a 38 μm filter and fixed by paraformaldehyde (0.5% final concentration). After 10-min of reaction, the samples were frozen and stored at −80 °C. Abundances of *Synechococcus*, picoeukaryotes, and *Prochlorococcus*-like cells were enumerated using Beckman Coulter's CytoFLEX S
110 Flow Cytometer (Zhou et al., 2021). Carbon biomasses of *Synechococcus*, picoeukaryotes, and *Prochlorococcus*-like cells were estimated using the converting factors of 101, 530, and 32 fg C cell L^{-1}, respectively (Garrison et al., 2000; Worden et al., 2004). Samples were prepared in triplicate.

We measured the abundances of ciliates and chain-forming diatom via an automated FlowCAM system (Portable Series FlowCAM). Dinoflagellates are also important at the Wanshan station but are difficult to be accurately quantified by
115 FlowCAM. The samples were screened by a 200 μm mesh to remove large particles. A volume of 300 mL sample was analyzed on Auto-image mode using a 300-μm flow cell and a flow rate of 2 ml min^{-1} (Anderson and Harvey, 2019; Haraguchi et al., 2018). Duplicate runs were pooled for each experiment. The results of FlowCAM were further validated by the inverted microscopic method. Briefly, seawater of 1000 ml was fixed with acidic Lugol's solution (1% final concentration) and stored in amber plastic bottles at room temperature. After pre-concentrated using the Utermöhl method
120 (Utermöhl, 1958), a 20 ml subsample was counted with an inverted microscope at 200×magnification. The biomass of

aloricate ciliate was estimated from biovolume using the conversion factor of 0.19 pg C μm^{-3} (Putt and Stoecker, 1989) with Tintinnid biomass using the equation: pg C= 444.5+ 0.053 × lorica volume (μm^3) (Verity and Langdon, 1984).

2.3 Setup of size-specific multi-treatment dilution experiments

125   The size-specific dilution experiment was carried out directly at a coastal pier 500 m away from the sampling site. The protocol of dilution experiments has been described in detail by Dong et al. (2018). Briefly, all the bottles, tubing, and carboys for the dilution experiment were soaked in 10% HCl for at least 24 h and rinsed with deionized water and *in situ* surface seawater successively before each experiment. Particle-free water was prepared by gravity filtered the prescreened seawater through a 0.2 μm filter. The whole seawater was gently poured into 2.4 L polycarbonate bottles containing specific

130   volumes of particle-free water to obtain a dilution series of 10%, 20%, 40%, 70%, and 100% whole seawater. Each dilution treatment was duplicated during the experiment. Ten incubation bottles were enriched with dissolved inorganic nutrients of 5 $\mu mol\ l^{-1}$ $NaNO_3$, 0.5 $\mu mol\ l^{-1}$ KH_2PO_4, and 5 $\mu mol\ l^{-1}$ Na_2SiO_3 to ensure the constant growth of phytoplankton (particularly to avoid nutrient limitation during winter). The amounts of nutrients are slightly lower than those used by Chen et al. (2009), given that our Wanshan station is relatively closer to the northern South China Sea than their site. There were two additional

135   bottles filled with the whole seawater served as controls without nutrient addition. All these bottles were tightly capped and incubated for 24 h in an incubator filled with the running surface seawater near the pier (with similar water temperature as the sampling site) and covered with a neutral density screen to mimic the *in situ* temperature and light at the station. Initial Chl-*a* concentrations of the diluted bottles were estimated from the whole seawater multiplied by the dilution factor, which has been verified by the direct measurements. Aliquots of 500 ml samples at the end of the 24 h culture were taken from

140   each bottle for Chl-*a* measurement.

2.4 Estimates of growth rate and grazing rate

Estimates of nutrient-enriched phytoplankton growth rate (μ_n, d^{-1}) and microzooplankton grazing rate (m, d^{-1}) for total phytoplankton community (Landry and Hassett, 1982) were calculated with least-square regression between the apparent

145   growth rates (ε_d, d^{-1}) and the dilution factors (d) as

$$\varepsilon_d = \frac{1}{t}\ln\left[\frac{Chl_d(t)}{Chl_d(0)}\right] = \mu_n - d \cdot m$$

$$\mu_0 = \varepsilon_{raw} + m$$

where, $Chl_d(0)$ and $Chl_d(t)$ are the initial and final concentrations of Chl-a for each dilution treatment (d) with t the incubation time (one day in our experiment). The natural growth rate (μ_0) is calculated as the sum of the apparent growth rate without nutrient enrichment (ε_{raw}) and the grazing rate (Landry et al., 1993).

For each phytoplankton size-class i (micro, nano, and pico, respectively), we have similar equations as

$$\varepsilon_d^i = \frac{1}{t}\ln\left[\frac{Chl_d^i(t)}{Chl_d^i(0)}\right] = \mu_n^i - d \cdot m_i$$

$$\mu_i = \varepsilon_{raw}^i + m_i$$

where, μ_i and μ_n^i are the natural and nutrient-enriched growth rates of size-class i with m_i the size-specific grazing rate. ε_{raw}^i and ε_d^i are the raw and nutrient nutrient-enriched apparent growth rates of size-class i.

2.5 Statistics Analysis

Statistical analyses were performed using software SPSS 14.0. Comparisons between environmental variables were conducted using reduced major axis model II regression with r representing the Pearson coefficient of correlation. A permutation test was carried out to determine the significance of the slopes and calculate the p-value. The level of $p<0.05$ was considered significant, with $p<0.01$ as strong significance. Following the One way independent measures ANOVA (one-way ANOVA), the significance of the difference between growth/grazing rates and zero was checked using Tukey's HSD test. Responses of the size-fractionated growth and grazing rates to varying environmental parameters were investigated by multivariate statistical analyses using CANOCO version 5.0. Redundancy analysis (RDA) was used to summarize relations between size-fractionated rates and environmental parameters once the length of the first gradient was satisfied by a linear justification.

3. Results

3.1 Temporal change of hydrodynamics in the study area

At the Wanshan station, there was a strong stratification induced by river discharge and seawater intrusion during the summer in contrast to the well-mixed water column during the winter (Fig S1). Despite a much higher seawater temperature, surface salinity was much lower in the summer (15.3±8.1) than in the winter (33.3±0.2), reflecting a stronger river discharge. The structure of the summer river plume was manifested by a layer of low salinity (7.2-24.4) surface water extending from the estuary to the inner shelf

Pronounced seasonal variations in temperature, salinity, river flow, and solar radiation were observed during the one-

year time-series study at the Wanshan station (Fig. 2A and 2B). The annually-averaged temperature is about 24.8±3.5ºC, varying from 19.0 to 28.5ºC (Fig. 2A). Salinity fluctuation at Wanshan was evidenced in response to the seasonal flood of freshwater runoff from the Pearl River. While a substantially low salinity (<26) showed up in June, August, and September 2018, there was a relatively higher salinity of ~33 found during the other months of the year. There was about 66% of the river discharge occurring in the wet season of April-September with a total flow rate of $82.7×10^3$ m^3 s^{-1}, which is about twice that in the dry season of October-March (total of $41.5×10^3$ m^3 s^{-1}) (Fig. 2B).

A strong negative correlation between the monthly flow rate of the Pearl River and the salinity at Wanshan (r=-0.82, n=12, p<0.01) was observed, which should indicate an essential role of river input on the temporal change of local hydrodynamics at the Wanshan station. Also, the flow rate was positively correlated with nitrate and silicate concentrations (Table S1), which may reflect a major source of nutrients to the Wanshan station from river discharge. There was an apparent seasonal change of solar radiation (Fig. 2B), with the lowest value in the winter (297.7 MJ m^{-2}) but the highest value in the summer (546.2 MJ m^{-2}). We also found periods of slightly reduced light intensity during August and May due to the cloud coverage. Solar radiation was positively correlated to temperature throughout the year ($r = 0.76$, n=12, p<0.01) but not with any other environmental parameters at our station (Table S1).

3.2 Temporal change of plankton ecosystem and biogeochemistry

Surface concentrations of nitrate ranged from 3.6 to 69.4 µmol L^{-1} (with an average of 25.3±23.7 µmol L^{-1}) (Fig. 2C). There were peaks of nitrate in June, September, January, and April during the one-year cycle, with the highest concentration of 64.8 µmol L^{-1} found in September. Nitrate concentration decreased dramatically in the late autumn, with the lowest 3.6 µmol L^{-1} found in December. Temporal variations of phosphate and silicate were generally in agreement with that of nitrate (Fig. 2C), which was confirmed by significant correlations between nitrate and phosphate ($r = 0.64$, n=12, p<0.05) and between phosphate and silicate ($r = 0.73$, n=12, p<0.01). The surface N/P ratios were very high at the Wanshan station (21.6-116.4), indicating a potential phosphorus deficiency compared to the Redfield ratio. Salinity showed strong negative correlations with both nitrate and silicate, which should reflect the impact of river discharge with an intense mixing between the eutrophic river water and the low-nutrient seawater at the Wanshan station. Meanwhile, we found no correlation between phosphate and salinity (Table S1).

There was a large seasonal change of total Chl-a varying from 0.33 to 8.1 µg L^{-1} during the study period (with an average of 1.9±2.2 µg L^{-1}). Consistent with those of nutrients, a generally higher total Chl-a was found during the summer with a maximum of 8.1µg L^{-1} in August. In contrast, a low Chl-a concentration of 1.0±0.3 µg L^{-1} was found among the other months of the year. For the size-fractioned Chl-a, the phytoplankton community was predominated by nano-cells (on average 60.4±14.5%) throughout the year, followed by pico- (22.4±7.5%) and micro-cells (17.2±14.5%), respectively. Also, there was a high Chl-a concentration and a high percentage of microphytoplankton showing up in June and August 2018

(Fig. 3A) when the total Chl-*a* concentration was high (Fig. 3B). A high percentage of micro-cells was also found in February and May 2019, although the total Chl-*a* was relatively low (Fig. 3B).

The abundance of diatom, dominant by chain-forming taxa (mainly *Skeletonema costatum* and *Staphylococcus spiralis*), varies substantially from undetectable to 23.8×10^5 cell L^{-1} during our study period (Fig. 4A). A seasonal change of diatom abundance was documented with a lower concentration in the winter but a high concentration in the summer. Consistent with that of the pico-sized Chl-*a* (Fig. 3A), there was a much higher picophytoplankton carbon biomass found in the summer than in the winter (Fig. 4B). Generally, *Synechococcus* dominated the picophytoplankton community most of the year, with an average abundance of $30.4\pm26.7 \times10^6$ cells L^{-1}. *Prochlorococcus*-like cells were mostly negligible through the one-year study (Fig. 4B) except for some months during the summer with high nutrients but low salinity (Fig. 2B and 2C). Microzooplankton at the Wanshan station were dominated by ciliates (mostly aloricate ciliates and Tintinnids; similar to Chen et al., 2009). There was a seasonal change of ciliates (Fig. 4C) with higher biomass found in July (4.6 µg C L^{-1}) and October (2.1 µg C L^{-1}).

3.3 Temporal change of phytoplankton growth and microzooplankton grazing rates

Figure S2 are the typical results of the size-specific dilution experiments (only two representative months are shown due to the space limitation). Generally, a significant linear relationship between apparent growth rate and the dilution factors was acquired during our monthly dilution experiments. However, the dilution method could not apply to the experimental results of July and October 2018 when a positive slope of the dilution curve was found together with a very high ratio of ciliates over the total Chl-*a* (Fig. 4C). The natural growth rates during these two months could be estimated from the undiluted treatment assuming a zero grazing rate as suggested by Calbet and Saiz (2013) when a trophic cascade occurs in the dilution experiment due to omnivorous ciliates feeding on smaller carnivores.

Results of all the monthly dilution experiments at the Wanshan station are shown in Fig. 5 and Table S2. There were apparent seasonal differences in both growth and grazing rates during our observation period. Generally, we found higher rates in summer than spring/winter for both phytoplankton growth and microzooplankton grazing. Phytoplankton natural growth rate varied from -0.34 to 2.96 d^{-1} with an average of 1.09 ± 0.95 d^{-1} during the one-year cycle (Fig. 5A). The negative rate of -0.34 d^{-1} was found in February with the lowest temperature and solar radiation, which however was barely different from zero (One-Way ANOVA, $p=0.24$). Temporal change of grazing rate (*m*) was much different from that of natural growth rate, with the highest rate of ~2.1 d^{-1} showing up in August (Fig. 5B). These were apparent decoupling between phytoplankton growth and microzooplankton grazing in August and September 2018.

Temporal variations of the size-fractioned growth and grazing rates generally followed the trends of total community with higher rates in the summer but lower rates in the winter/spring. There was no general difference found among the natural growth rates of three phytoplankton size classes ($p>0.05$) except April and May 2019. An elevated growth of micro-

cells but a reduced growth of nano-cells was found in April 2019 compared to that of pico-cells (Fig. 5A). Also, there were large negative natural growth rates of nanophytoplankton during April and May 2019 (significantly different from zero, One-Way ANOVA, $p<0.01$), further discussed in the next section. There was an increase of microzooplankton grazing on pico-cells in September 2018 and June 2019 but on large cells in November and February 2018 (Fig. 5B). There were substantial increases in nutrient-enriched growth rate (μ_n) found in June, September, January, and April (Fig. 5C), which was well consistent with the elevated nutrient concentrations in these months shown previously (Fig. 2C). Generally, the annual average of the nutrient-enriched growth rate (1.68 d^{-1}) was higher than that of the natural growth rate (1.22 d^{-1}), indicating a nutrient deficiency of phytoplankton even in this highly eutrophic system.

4. Discussion

4.1 What controls the seasonal change of phytoplankton production?

Phytoplankton growth in the ocean can be influenced by several factors, such as temperature, light, nutrients, and community structure (e.g. Li et al., 2010). Temperature has been known as an important driver for phytoplankton growth (e.g. Eppley, 1972). The temperature effect on phytoplankton growth at the Wanshan station was evidenced by a strong correlation of the community growth rate (μ_0) with the temperature ($r=0.96$, $n=6$, $p<0.01$) during the period of October to April when salinity (and nutrients) relatively less fluctuated. The effect of light on phytoplankton growth at the Wanshan station was similar to that of temperature given the strong correlation between solar radiation and temperature.

Besides temperature and light, dissolved nutrients can also affect phytoplankton growth at the Wanshan station. During June-September 2018 when the water temperature was relatively constant, the community growth rate showed strong correlations with nutrients ($r=0.95$, $n=4$, $p<0.01$ for nitrate) but not with other parameters, such as light and grazing. Nutrient limitation index (μ_0/μ_n) can be used to assess the degree of nutrient shortage for phytoplankton growth with a lower value of less than one indicating a stronger nutrient limitation. The mean nutrient limitation index of μ_0/μ_n for the whole community was about 0.9±0.2 at the Wanshan station, suggesting that phytoplankton here was generally not limited by nutrients. This could well explain the very similar patterns found between the nutrient-enrich growth rates (μ_n) and the natural growth rate (μ_0) for the total phytoplankton community. A negative correlation of the natural growth rate with salinity during the one-year cycle could be attributed to nutrients given the tight relationship between salinity and nutrients at the Wanshan station. We can simply divide the environmental variables into two independent groups based on their correlations with each other (Table S1), including temperature (light) and nutrient (salinity). The slow growth of the phytoplankton community (together with a low Chl-a level of <1 μg L^{-1}) in the winter was consistent with the low temperature and the low nutrient conditions. Thus, the interplay between the two groups of independent factors may be responsible for the seasonal change of phytoplankton growth during the one year.

It is surprising to find negative natural growth rates of nanophytoplankton during April and May 2019. The natural growth of nanophytoplankton was likely limited by nutrients since its growth was well promoted during the nutrient-enriched treatments (Fig. 5C). Moreover, a substantially high N/P ratio during these two months suggested that phosphate was largely deficient relative to nitrate in these waters. Phosphorus limitation of nanophytoplankton may infer a disadvantage of nano-cells in competing for phosphorus resources with micro- and pico-cells. Recent studies suggested that picophytoplankton could store and liberate poly-phosphate to support high productivity in a low phosphate environment (Li et al., 2019). Also, it has been well-known that microphytoplankton could use dissolved organic phosphorus to sustain growth and maintain a sufficient amount of biomass under P-deplete conditions (Girault et al., 2013). However, nanophytoplankton by itself tends to be limited by phosphorus compared to other size phytoplankton when a high N/P ratio was observed. Therefore, a substantial difference in natural growth rate among the three size classes during April 2019 should reflect their different tolerance capacity to P-deficiency.

We use redundancy analyses (RDA) to explore the factors controlling the size-fractionated growths of phytoplankton over the annual cycle (Fig. 6A). The first axis explains ~69.63% of the variance in natural growth rate with the second axis for ~13.1%, which should guarantee the validation of the RDA method in our study area. The statistical approach highlighted several important factors in driving the observed seasonal change in the size-fractionated phytoplankton growth rates, including temperature, light, and nutrients (Fig. 6A). Microphytoplankton growth seemed more influenced by phosphate than by other factors. This is consistent with the phosphorus control of large phytoplankton growth commonly found in the frontal zones near Wanshan (Li et al., 2018). A higher maximal growth rate together with a larger half-saturation constant will be an advantage for microphytoplankton growth (Dong et al., 2018) in response to an increase of P loading from river inputs in a P-deficient system with extremely high N/P ratios. In contrast, picophytoplankton growth was primarily controlled by nitrate and temperature. This finding is also in good agreement with the previous reports that the growth rates of *Synechococcus* and picoeukaryotes would generally increase with temperature and nitrate concentrations in the coastal NSCS (Chen et al., 2014). Interestingly, we found nanophytoplankton was more controlled by light than the other factors. It has been suggested that phytoplankton growth on the west coast of Spitsbergen can be driven by solar irradiance on seasonal and inter-annual scales, as the cycles of warming and freshwater discharge in the coastal regions are primarily controlled by solar radiation (van de Poll et al., 2021). The dominant species of nanophytoplankton in the PRE region are small chain-forming diatoms, such as *S. costatum* and *Thalassiosira spp*, with chain lengths (or diameters of cell colonies) of less than 20 μm (Li et al., 2013). These small-sized chain-forming diatoms (nanophytoplankton) can grow first when light becomes not limiting in the eutrophic environment and followed by larger species as nutrients are consumed (e.g. Guillard and Kilham, 1977).

4.2 Drivers for seasonal variability in microzooplankton grazing

We address the temporal change in the feeding strategy of microzooplankton by focusing on their grazing rates on total phytoplankton community (m) as well as on various phytoplankton size-classes (m_{micro}, m_{nano}, and m_{pico}). We present evidence for the size-selective prey preference of microzooplankton on small autotrophs, which may have a great impact on the temporal dynamics of the plankton community in the coastal ocean.

Generally, microzooplankton grazing (m) at the Wanshan station varied substantially on an annual cycle in response to change in phytoplankton concentration and composition. Surprisingly, we find a zero grazing rate in July when the temperature is high, despite a positive correlation between community grazing rate and temperature ($r=0.62$, $n=12$, $p<0.05$). In addition, extensive modulation of grazing rate was observed during June-September 2018, when the water temperature was mostly constant. The temperature effect on microzooplankton grazing may not be straightforward (Rose and Caron, 2007). It should be pointed out that the temperature sensitivity of microzooplankton grazing could have been masked in our monthly data given the large fluctuation of grazing rate over a wide range of Chl-a levels. Though other environmental factors such as light and nutrients may likely be relevant to grazing rates in the coastal ocean (Chen et al., 2009), these relationships were not supported by our direct linear regression analyses at the Wanshan station (Table S1).

Our results support the density-dependent prey ingestion kinetics found in laboratory culture experiments (e.g. Holling, 1959), as evidenced by a significant correlation of the community grazing rate with the total phytoplankton Chl-a concentration ($r=0.82$, $n=12$, $p<0.01$). Based on the classic *Holling II* grazing model, a positive correlation between microzooplankton grazing rate and phytoplankton standing stock may occur during non-saturated feeding (Dong et al., 2018). However, size-dependent selectivity of microzooplankton grazers on phytoplankton prey can affect the community grazing activity resulting in decoupling between resident grazers and preys (Poulin and Franks, 2010). In this case, grazer biomass alone may not accurately reflect community grazing rates (Menden-Deuer et al., 2018). This was likely the case at the Wanshan station when the community grazing rate was poorly explained by the ciliate biomass.

Redundancy analyses were also employed to address the linkages between the size-fractionated grazing rates and the environmental variables (Fig. 6B), with the first axis accounting for ~69.4 % and the second axis for ~12.8 % of the variance. The grazing mortality rate of nano-cells was more correlated to picoplankton biomass as well as all the size-fractionated Chl-a concentrations than the other factors. This result is consistent with the significant correlation between community grazing rate and total Chl-a mentioned in the previous paragraph since nano-phytoplankton was the dominant size-class at the Wanshan station. Interestingly, the grazing rate on micro-cells was negatively influenced by the ciliate abundance. A reverse correlation of ciliate with the grazing rate (m_{micro}) could be explained by selective grazing of microzooplankton on nano- and pico-phytoplankton community (this will be further discussed in the next few paragraphs). Finally, we found a negative correlation of salinity with the grazing rate on picophytoplankton. It has been suggested that small herbivores, such as heterotrophic nano-flagellates, would preferentially graze on picoplankton (Christaki et al., 2001), although they are more sensitive to salinity change in mesotrophic coastal waters (Jolliff et al., 2012). A negative correlation of salinity with the abundance of smaller zooplankton in the Jiaozhou Bay of the South Yellow Sea has been attributed to the discharge of eutrophic freshwater (Wang et al., 2020). This may likely be also true at the Wanshan station given the negative correlation

between salinity and nutrients. Therefore, the input of low-salinity/high-nutrient water stimulates phytoplankton growth and thus the growth of zooplankton grazing on them.

We found that microzooplankton grazing was an important pathway for phytoplankton loss, although there was a large difference among the three size classes (Fig. 7). On average, microzooplankton consumed ~38% of microphytoplankton production (r=0.62, n=21, p<0.01), much lower than that of ~72% for nanophytoplankton (r=0.63, n=15, p<0.01) and ~60% for picophytoplankton (r=0.75, n=17, p<0.01) (Fig. 7). Our results for nano- and picophytoplankton are consistent with those of 60-75% reported in the global ocean (Calbet and Landry, 2004). A low value for microphytoplankton suggests that additional processes not captured by the dilution technique, such as mesozooplankton grazing, may be important for phytoplankton loss. Mesozooplankton (>200 µm) prefer large phytoplankton (such as dinoflagellates and diatoms) for prey although their contribution to grazing is typically less than microzooplankton (Steinberg and Landry, 2017; Calbet and Landry 1999; Karu et al., 2020). Mesozooplankton generally consumes ~12% of the primary production (Calbet 2001; Liu et al., 2010) with a large variability of 0.7-31% in the coastal waters near the PRE (Chen et al., 2015). Higher grazing on nano- and pico-cells compared to micro-cells may indicate size-selective feeding of microzooplankton on small cells. This result is contradicted to the previous finding of no size-selective grazing in the coastal waters west of Hong Kong (Lie and Wong, 2010). Meanwhile, it is consistent with our finding of a high abundance of large chain-forming diatoms at the Wanshan station, which can effectively avoid grazing by microzooplankton and copepod due to their chain length plasticity (Bergkvist et al., 2012).

Monthly grazing impact (m_i/μ_i) at the Wanshan station reveals a seasonal change of size-selective prey preference of microzooplankton with increased grazing on nanophytoplankton during the winter-spring period (Fig. S3). Large aloricate ciliates (30-50 µm), the dominant micrograzers in our system, are the major consumers of nanoplankton (Bernard and Rassoulzadegan, 1990). Increased ingestion of aloricate ciliates on phototrophic nanoflagellate during the winter with lower nanoplankton biomass and productivity has been reported in the coastal waters off Chile (Vargas and Martinez, 2009). Our results are also consistent with the previous finding in the Southern Ocean with microzooplankton preferentially grazing on the nano- and pico-phytoplankton during the winter when the community was dominated by small cells (Froneman and Perissinotto, 1996). Alternatively, it has also been suggested that an increase of grazing on small autotrophs may be caused by microzooplankton growth due to the artifact of removing mesozooplankton from the incubations (Schmoker et al., 2013; Calbet and Saiz, 2013). Meanwhile, this effect should be negligible here since mesozooplankton was barely present in our 200-µm screen during the one-year field study.

A seasonal change in size-selective feeding of microzooplankton may be crucial for understanding food web dynamics and the carbon cycle of the coastal ocean. It has been well recognized that temporal change of phytoplankton community structure can be regulated by size-selective herbivory of microzooplankton (Strom et al., 2007; Haraguchi et al., 2018). In addition, an enhanced export production may occur when large phytoplankton such as diatoms can escape from grazing by micrograzers due to size-selective prey preference on small cells (e.g. Froneman and Perissinotto 1996). Furthermore, nutrient recycling within the microbial food web can be influenced by selective grazing of microplankton on heterotrophic

bacterioplankton (Christaki et al., 2001; Unrein et al., 2007). On the other hand, our results may be also important for ecosystem and biogeochemical modeling. Previous results suggest that inaccurate representative of microzooplankton grazing and their prey selection can cause deficiencies of these models and cast doubts on the results of their predictions (e.g. Li et al., 2011; Sailley et al., 2015). In this sense, our finding of seasonal variability of size-selective grazing and their controlling factors should be crucial for not only the parameterization of grazing models but also the prediction of the shifts in the plankton community structure in response to future climate change.

5. Conclusion

By statistically analyzing the relationships between plankton rates and environmental variables through one year at a coastal station outside a eutrophic estuary, we explore the underlying mechanisms controlling the monthly change of phytoplankton growth and microzooplankton grazing. We find that the temporal change in environmental parameters including light, temperature, nitrate, and phosphate could have distinct impacts on the growth of different phytoplankton size classes. Also, the grazing mortalities of various phytoplankton size classes could be related to different factors, including salinity, phytoplankton standing stock, and ciliate abundance. Moreover, selective grazing of microzooplankton on small cells may be important for maintaining a high abundance of large chain-forming diatoms in this eutrophic system. In summary, our results suggested that both the bottom-up and the top-down factors can interact together to control the growth and grazing mortality of phytoplankton of various sizes.

Our one-year time-series study should offer valuable insights into the seasonal change and the interplay of various environmental factors in controlling plankton population dynamics in the studied area. In addition, our findings of seasonal variabilities in plankton rates and their regulating mechanisms may be important for ocean biogeochemical modeling to accurately account for the carbon flows within the microbial food web and to better predict biological responses to future climate change.

ASSOCIATED CONTENT

AUTHOR INFORMATION

CORRESPONDING Author

Email: qianli@scsio.ac.cn

ORCID

Qian P Li: 0000-0002-9846-3243

Present Address

South China Sea Institute of Oceanology, 164 West Xingang Road, Guangzhou,

China 510301

Data availability. Some of the data used in the present study are available in the Supplement. Other data analyzed in this article are available at the National Earth System Science Data Center, China (http://data.scsio.ac.cn/metaData-detail/1405396650095489024).

Author Contributions. YD conducted the investigation, methodology, Software and writing original draft. QPL provided supervision, visualization, investigation, conceptualization, methodology, data curation, reviewing and editing and funding acquisition. ZCW, YPS, ZJL, ZMG, ZZW and YCC helped investigation. All authors have given approval to the final version of the manuscript.

Competing interests. The authors declare no competing financial interest.

Acknowledgements. We would like to thank Mr. Guanghui Li for field assistance, as well as editor and reviewers for constructive comments.

Finanical support. This study was supported by the National Natural Science Foundation of China (41906132), the Guangdong Province Special Supporting Plan for Leading Talent (2019TX05H216), the Key Special Project for Introduced Talents Team of Southern Marine Science and Engineering Guangdong Laboratory (Guangzhou) (GML2019ZD0305).

REFERENCES

Anderson, S. R., and Harvey, E. L.: Seasonal variability and drivers of microzooplankton grazing and phytoplankton growth in a subtropical estuary, Front. Mar. Sci., 6, 174, https://doi.org/10.3389/fmars.2019.00174, 2019.

Bergkvist, J., Thor, P., Jakobsen, H. H., Wängberg, S., and Selander, E.: Grazer-induced chain length plasticity reduces grazing risk in a marine diatom, Limnol. Oceanogr., 57, 318-324, https://doi.org/10.4319/lo.2012.57.1.0318, 2012.

Bernard, C., and Rassoulzadegan, F.: Bacteria or microflagellates as a major food source for marine ciliates: possible implications for the microzooplankton, Mar. Ecol. Prog. Ser., 64, 147-155, https://doi.org/10.3354/meps064147, 1990.

Calbet, A., and Landry, M. R.: Mesozooplankton influences on the microbial food web: Direct and indirect trophic interactions in the oligotrophic open ocean, Limnol. Oceanogr., 6, http://doi.org/10.4319/lo.1999.44.6.1370, 1999.

Calbet, A.: Mesozooplankton grazing effect on primary production: A global comparative analysis in marine ecosystems, Limnol. Oceanogr., 7, http://doi.org/ 10.4319/lo.2001.46.7.1824, 2001.

Calbet, A., and Landry, M. R.: Phytoplankton growth, microzooplankton grazing, and carbon cycling in marine systems, Limnol. Oceanogr., 49, 51-57, https://doi.org/10.4319/lo.2004.49.1.0051, 2004.

Calbet, A., and Saiz, E.: Effects of trophic cascades in dilution grazing experiments: from artificial saturated feeding responses to positive slopes, J. Plankton Res., 35, 1183-1191, https://doi.org/10.1093/plankt/fbt067, 2013.

Chen, B. Z., Liu, H. B., Landry, M. R., Chen, M. R., Sun, J., Shek, L., Chen, X., and Harrison. P. J.: Estuarine nutrient loading affects phytoplankton growth and microzooplankton grazing at two contrasting sites in Hong Kong coastal waters, Mar. Ecol. Prog. Ser., 379, 77-90, https://doi.org/10.3354/meps07888, 2009.

Chen, B. Z, Laws, E. A., Liu, H. B., and Huang, B. Q.: Estimating microzooplankton grazing half-saturation constants from dilution experiments with nonlinear feeding kinetics, Limnol. Oceanogr., 59, 639-644, https://doi.org/10.4319/lo.2014.59.3.0639, 2014.

Chen, M. R., Liu, H. B, Song, S. Q., and Sun, J.: Size-fractionated mesozooplankton biomass and grazing impact on phytoplankton in northern South China Sea during four seasons, Deep-Sea Res. II., 117, 108-118, https://doi.org/10.1016/j.dsr2.2015.02.026, 2015.

Christaki, U., Giannakourou, A., Wambeke, F. V., and Grégori, G.: Nanoflagellate predation on auto-and heterotrophic picoplankton in the oligotrophic Mediterranean Sea, J. Plankton Res., 23, 1297-1310, https://doi.org/10.1093/plankt/23.11.1297, 2001.

Cloern, J. E., Foster, S. Q., and Kleckner, A.E.: Phytoplankton primary production in the world's estuarine-coastal ecosystem, Biogeosciences, 11, 2477e2501, https://doi.org/10.5194/bg-11-2477-2014, 2014.

Dong, Y., Li, Q. P., Liu, Z. J., Wu, Z. C., and Zhou, W. W.: Size-dependent phytoplankton growth and grazing in the northern South China Sea, Mar. Ecol. Prog. Ser., 599, 35-47, https://doi.org/10.3354/meps12614, 2018.

Eppley, R. W.: Temperature and phytoplankton growth in the sea, Fish. Bullet., 70(4), 1063-1086, 1972.

Froneman, P., and Perissinotto, R.: Microzooplankton grazing in the Southern Ocean: implications for the carbon cycle, Mar. Ecol., 17, 99-115, https://doi.org/10.1111/j.1439-0485.1996.tb00493.x, 1996.

Gan, J. P., Lu, Z. M., Dai, M. H., Cheung, A. Y. Y., Liu, H. B., and Harrison, Paul.: Biological response to intensified upwelling and to a river plume in the northeastern South China Sea: A modeling study, J. Geophys. Res., 115, C09001, https://doi.org/10.1029/2009JC005569, 2010.

Garrison, D. L., Gowing, M. M., Hughes, M. P., Campbell L., Caron D. A., Dennett, M. R., Shalapyonok, A., Olson, R. J., Landry, M. R., Brown, S. L., Liu, H. B., Azam, F., Steward, G. F., Ducklow, H. W., Smith, D. C.: Microbial food web structure in the Arabian Sea: a US JGOFS study, Deep-Sea Res. II., 47, 1387-1422, https://doi.org/10.1016/S0967-0645(99)00148-4, 2000.

Girault, M., Arakawa, H., and Hashihama, F.: Phosphorus stress of microphytoplankton community in the western subtropical North Pacific, J. Plankton Res., 35(1), 146-157, https://doi.org/10.1093/plankt/fbs076, 2013.

Guillard, R. R. L. and Kilham, P.: The ecology of marine plankton diatoms, in: The Biology of Diatoms, editd by: Werner, D., University California Press, Berkeley, 372-469, 1977.

Hansen, H. P., and Koroleff. F.: Determination of dissolved inorganic phosphate, in: Methods of seawater analysis, edited by: Grasshoff, K., Kremling, K., and Ehrhardt, M., John Wiley and Sons. 159-228, https://doi.org/10.1002/9783527613984.ch10, 1999.

Haraguchi, L., Jakobse, H. H., Lundholm, N., and Carstensen, J.: Phytoplankton community dynamic: a driver for ciliate trophic strategies, Front. Mar. Sci., 5, 272, http://doi.org/10.3389/fmars.2018.00272, 2018.

Holling, C. S.: Some characteristics of simple types of predation and parasitism, The canadian entomologist, 91, 385-398, 1959.

Ichinotsuka, D., Ueno, H., and Nakano, S.: Relative importance of nanoflagellates and ciliates as consumers of bacteria in a coastal sea area dominated by oligotrichous Strombidium and Strobilidium, Aquat. Microb. Ecol., 42, 139-147, https://doi.org/10.3354/ame042139, 2006.

Jolliff, J. K., Smith, T. A., Barron, C.N., deRada, S., Anderson, S. C., Gould, R. W., Arnone, R.: The impact of coastal phytoplankton blooms on ocean−atmosphere thermal energy exchange: Evidence from a two−way coupled numerical modeling system, Geophys. Res. Lett., 39, L24607, https://doi.org/10.1029/2012GL053634, 2012.

Karu, F., Kobari, T., Honma, T., Kanayama, T., Suzuki, K., Yoshie, N., and Kume, G.:Trophic sources and linkages to support mesozooplankton community in the Kuroshio of the East China Sea, Fish. Oceanogr., 29, 442–456, https://doi.org/10.1111/fog.12488, 2020.

Landry, M. R., and Hassett, R. P.: Estimating the grazing impact of marine micro-zooplankton, Mar. Biol., 67, 283-288, https://doi.org/10.1007/bf00397668, 1982.

Landry, M. R., Monger, B. C., and Selph, K. E.: Time-dependency of microzooplankton grazing and phytoplankton growth in the subarctic Pacific, Prog. Oceanogr., 32, 205-222, https://doi.org/10.1016/0079-6611(93)90014-5, 1993.

Landry, M. R., Ohman, M. D., Goericke, R., Stukel, M. R., and Tsyrklevich, K.: Lagrangian studies of phytoplankton growth and grazing relationships in a coastal upwelling ecosystem off Southern California, Prog. Oceanogr., 83, 208-216, https://doi.org/10.1016/j.pocean.2009.07.026, 2009.

Li, J., Plouchart, D., Zastepa, A. and Dittrich, M.: Picoplankton accumulate and recycle polyphosphate to support high primary productivity in coastal Lake Ontario, Sci. Rep., 9, 19563, https://doi.org/10.1038/s41598-019-56042-5, 2019.

Li, L., Lv, S.H., Jiang, T., Li. X.: Seasonal variation of size-fractionated phytoplankton in the Pearl River estuary, Chinese Sci. Bull., 58, 2303-2314, https://doi.org/10.1007/s11434-013-5823-1, 2013.

Li, Q. P., Franks, P. J. S. Landry M. R., Goericke R., and Taylor, A. G.: Modeling phytoplankton growth rates and chlorophyll to carbon ratios in California coastal and pelagic ecosystems, J. Geophys. Res., 115, G04003, https://doi.org/10.1029/2009JG001111, 2010.

Li, Q. P., Franks, P. J. S. Landry M. R.: Microzooplankton grazing dynamics: parameterizing grazing models with dilution experiment data in the Southern California Ecosystem, Mar. Ecol. Prog. Ser., 438, 59-69, https://doi: 10.3354/meps09320, 2011.

Li, Q. P., Franks, P. J. S., Ohman, M. D., and Landry, M. R.: Enhanced nitrate fluxes and biological processes at a frontal zone in the southern California current system, J. Plankton Res., 34, 790-801, https://doi.org/10.1093/plankt/fbs006, 2012.

Li, Q. P., Zhou, W. W., Chen, Y. C., and Wu, Z. C.: Phytoplankton response to a plume front in the northern South China Sea, Biogeosciences, 15, 2551-2563, https://doi.org/10.5194/bg-15-2551-2018, 2018.

Lie, A. A. Y., and Wong, C. K.: Selectivity and grazing impact of microzooplankton on phytoplankton in two subtropical semi-enclosed bays with different chlorophyll concentrations, J. Exp. Mar. Biol. Ecol., 390(2), 149-159, http://doi.org/10.1016/j.jembe.2010.05.001, 2010.

Liu, H., Chen, M., Suzuki, K., Wong, C. K., and Chen, B.: Mesozooplankton selective feeding in subtropical coastal waters as revealed by HPLC pigment analysis, Mar. Ecol. Prog. Ser., 407, 111-123, https://doi.org/10.3354/meps08550, 2010.

Liu, K. K., Chao, S. Y., Shaw, P. T., Gong, G. C., Chen, C. C., and Tang, T. Y.: Monsoon-forced chlorophyll distribution and primary production in the South China Sea: observations and a numerical study, Deep Sea Res. I., 49, 1387–1412, http://doi.org/10.1016/S0967-0637(02)00035-3, 2002.

Menden-Deuer, S., Lawrence, C., and Franzè, G.: Herbivorous protist growth and grazing rates at in situ and artificially elevated temperatures during an Arctic phytoplankton spring bloom, PeerJ, 6, e5264. https://doi.org/10.7717/peerj.5264, 2018.

Parsons, T. R, Maita, Y., and Lalli, C. M.: A Manual of Chemical and Biological Methods for Seawater Analysis, Elsevier, New York, 1984.

Poulin, F. J., and Franks, P. J. S.: Size-structured planktonic ecosystems: constraints, controls and assembly instructions, J. Plankton Res., 32, 1121-1130, https://doi.org/10.1093/plankt/fbp145, 2010.

Putt, M. and Stoecker, D. K.: An experimentally determined carbon:volume ration for marine "oligotrichous" ciliates from estuarine and coastal waters, Limnol. Oceanogr., 34, 1097–1103, 1989.

Rose, J. M., and Caron, D. A.: Does low temperature constrain the growth rates of heterotrophic protists? Evidence and implications for algal blooms in cold waters, Limnol. Oceanogr., 52, 886-895. https://doi.org/10.4319/lo.2007.52.2.0886, 2007.

Sailley, S. F., Polimene, L., Mitra, A., Atkinson, A., and Allen, J. I.: Impact of zooplankton food selectivity on plankton dynamics and nutrient cycling, J. Plankton Res., 37(3), 519-529, https://doi.org/10.1093/plankt/fbv020, 2915.

Schmoker, C., Hernandez-Leon, S., and Calbet, A.: Microzooplankton grazing in the oceans: impacts, data variability, knowledge gaps and future directions, J. Plankton Res., 35, 691-706, https://doi.org/10.1093/plankt/fbt023, 2013.

Steinberg, D. K., and Landry, M. R.: Zooplankton and the ocean carbon cycle, Annu. Rev. Mar. Sci., 9, 413-444, https://doi.org/10.1146/annurev-marine-010814-015924, 2017.

Strom, S. L., Macri, E. L., and Olson, M. B.: Microzooplankton grazing in the coastal Gulf of Alaska: Variations in top-down control of phytoplankton, Limnol. Oceanogr., 52, 1480-94, https://doi.org/10.4319/lo.2007.52.4.1480, 2007.

Unrein, F., Massana, R., Alonso-Sáez, L., and Gasol, J. M.: Significant year-round effect of small mixotrophic flagellates on bacterioplankton in an oligotrophic coastal system, Limnol. Oceanogr., 52(1), 456-469, https://doi.org/10.4319/lo.2007.52.1.0456, 2007.

Utermöhl, H.: Zur vervolkomnung der quantitative Phytoplankton-Methodik. Mitteillung Internationale Verhandlungen Limnologie, 9, 1-38, https://doi.org/10.1080/05384680.1958.11904091, 1958.

van de Poll, W. H., Maat, D. S., Fischer, P., et al.: Solar radiation and solar radiation driven cycles in warming and freshwater discharge control seasonal and inter-annual phytoplankton chlorophyll a and taxonomic composition in a high Arctic fjord (Kongsfjorden, Spitsbergen), Limnol. Oceanogr., 66, 1221-1236, https://doi.org/10.1002/lno.11677, 2021.

Vargas, C. A., Martínez, R. A.: Grazing impact of natural populations of ciliates and dinoflagellates in a river-influenced continental shelf, Aquat. Microb. Ecol. 56:93-108, https://doi.org/10.3354/ame01319, 2009.

Verity, P. G. and Langdon, C.: Relationships between lorica volume, carbon, nitrogen and ATP content of tintinnids in Narragansett Bay, J. Plankton Res., 6, 859–868, 1984.

Wang, W. C., Sun, S., Sun, X., Zhang, G. T., and Zhang, F.: Spatial patterns of zooplankton size structure in relation to environmental factors in Jiaozhou Bay, South Yellow Sea, Mar. Pollut. Bull., 150, 110698, https://doi.org/10.1016/j.marpolbul.2019.110698, 2020.

Worden, A. Z., Nolan, J. K., and Palenik B.: Assessing the dynamics and ecology of marine picophytoplankton : The importance of the eukaryotic component, Limnol. Oceanogr., 49(1), 168-179, https://doi.org/10.4319/lo.2004.49.1.0168, 2004.

Wu, Z. C., and Li, Q. P. Spatial distributions of polyunsaturated aldehydes and their biogeochemical implications in the Pearl River Estuary and the adjacent northern South China Sea, Prog. Oceanogr., 147, 1-9, https://doi.org/10.1016/j.pocean.2016.07.010, 2016.

Zhou, W. W., Li, Q. P., and Wu, Z. C. Coastal phytoplankton responses to atmospheric deposition during summer, 555 Limnol. Oceanogr., 66(4), 1298-1315, https://doi.org/10.1002/lno.11683, 2021.
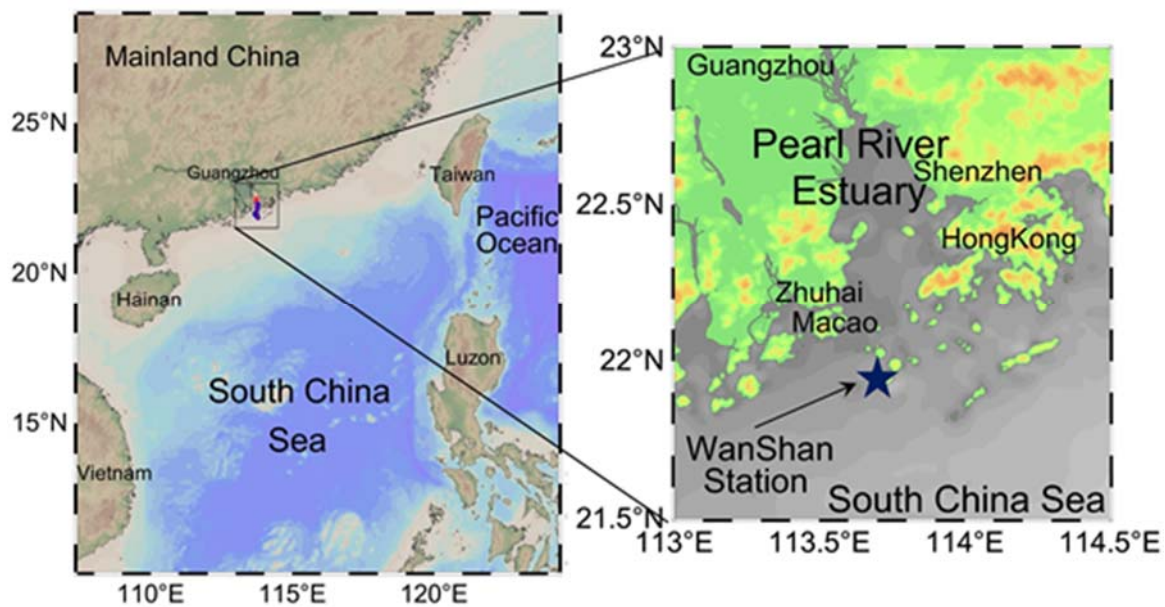
560

Figure 1: Geographic map of the Pearl River Estuary and the adjacent northern South China Sea. The filled star in the enlarged panel is the monthly timeseries station (21.9°N, 113.8°E) near Wanshan Island from June 2018 to June 2019.
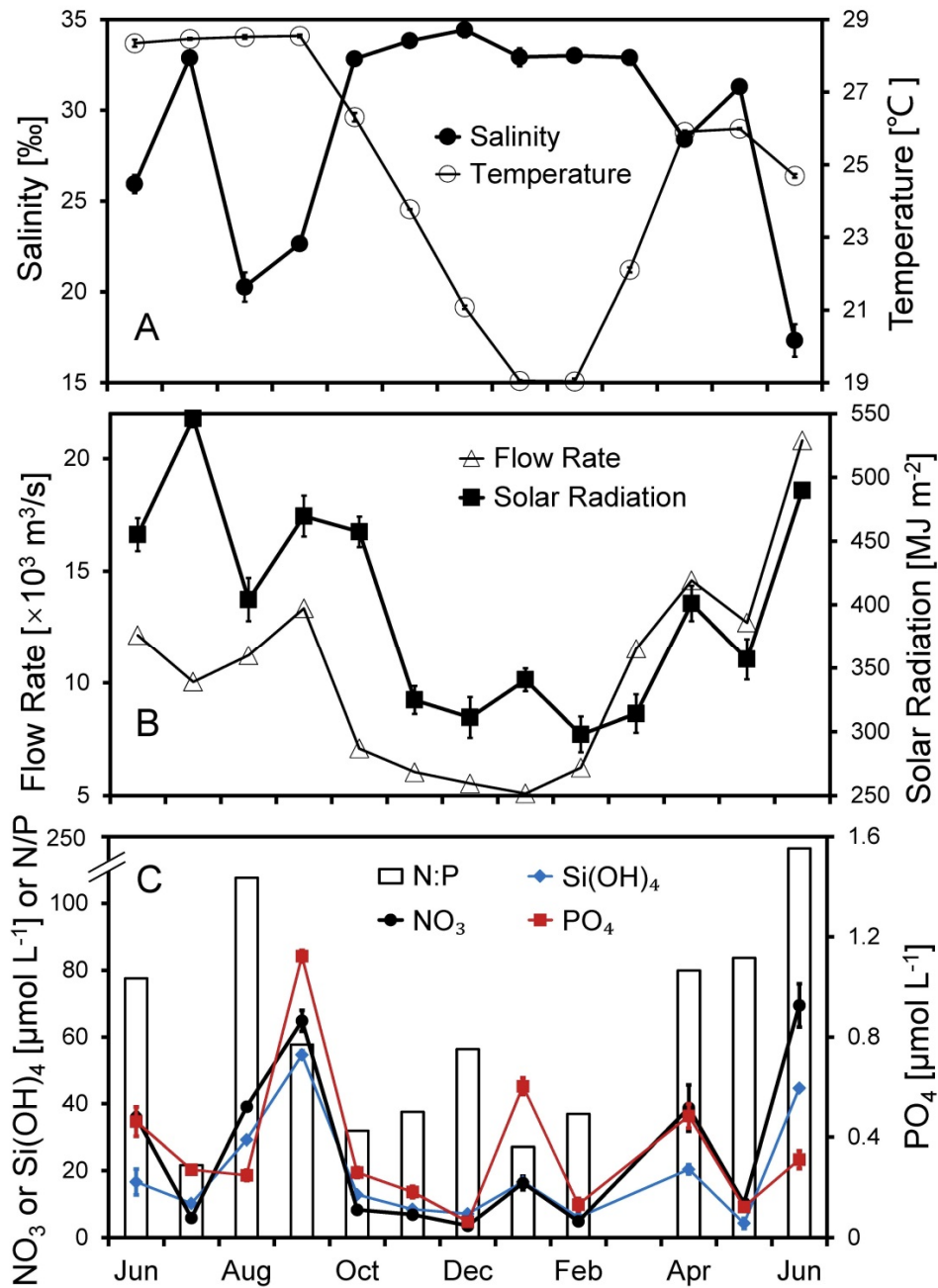
Figure 2: Temporal variations of (A) temperature, salinity, (B) flow rate, solar radiation, (C) nitrate, silicate, phosphate, and N/P ratio of the surface water at the Wanshan station from June 2018 to June 2019. Error bars are standard deviations.
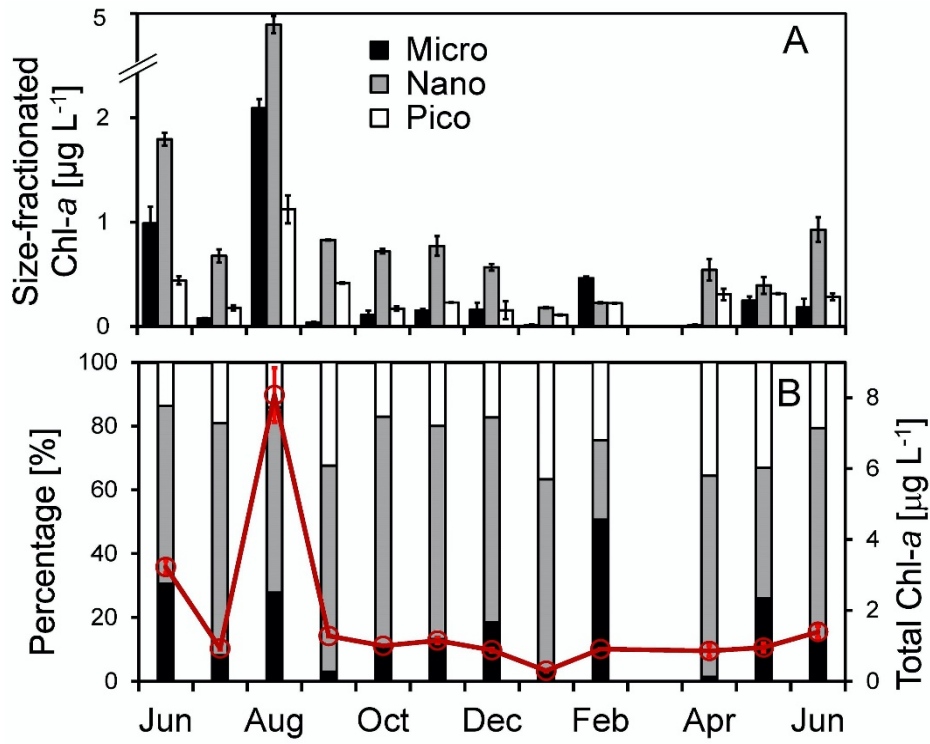
Figure 3: Temporal change of (A) size-fractionated chlorophyll-*a* concentrations of micro-, nano-, and pico-phytoplankton as well as (B) the total chlorophyll-*a* concentration (red circles and lines) and the size-fractionated percentages (columns) at the Wanshan station from June 2018 to June 2019. Error bars are standard deviations.

570
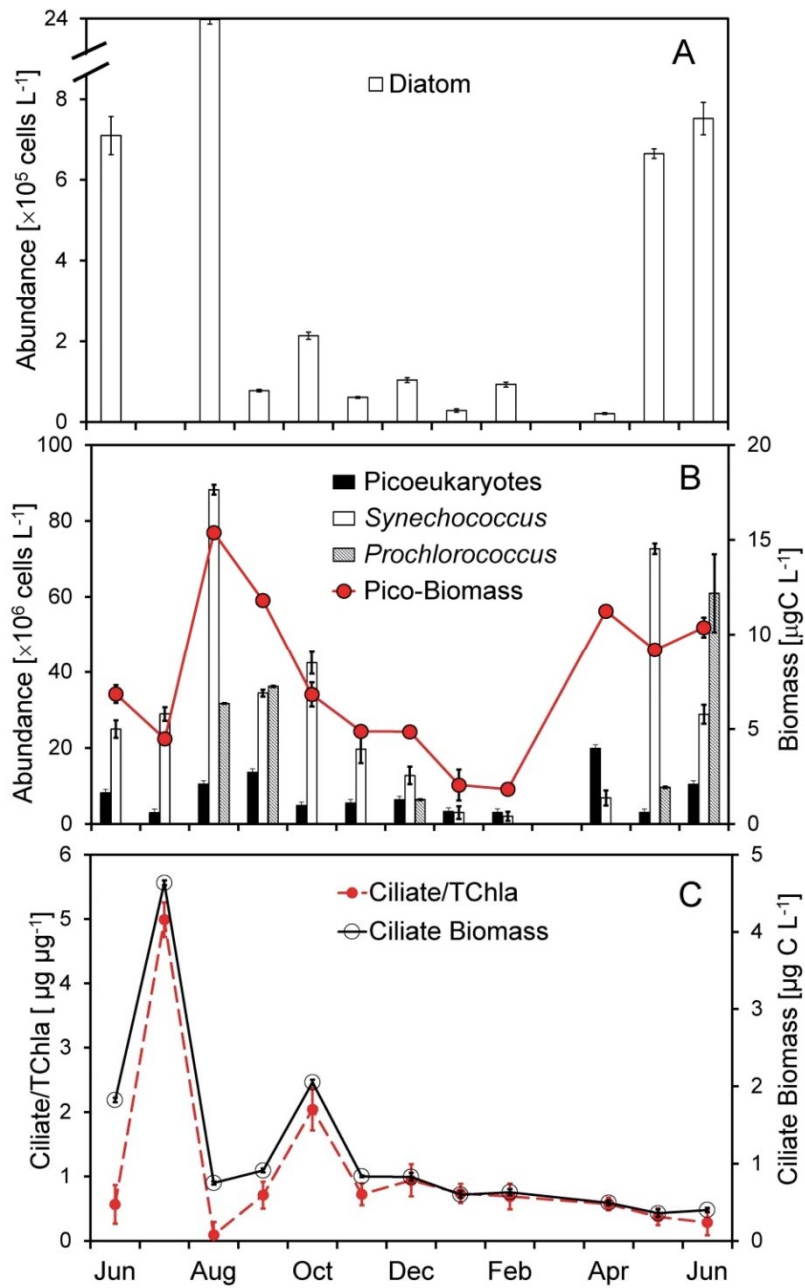
Figure 4: Temporal changes of (A) diatom abundance, (B) *Synechococcus* and pico-eukaryotes abundances, total picophytoplankton biomass, and (C) ciliate biomass and the ciliate-to-chlorophyll ratio of the surface water at the Wanshan station from June 2018 to June 2019. Error bars are standard deviations.

575
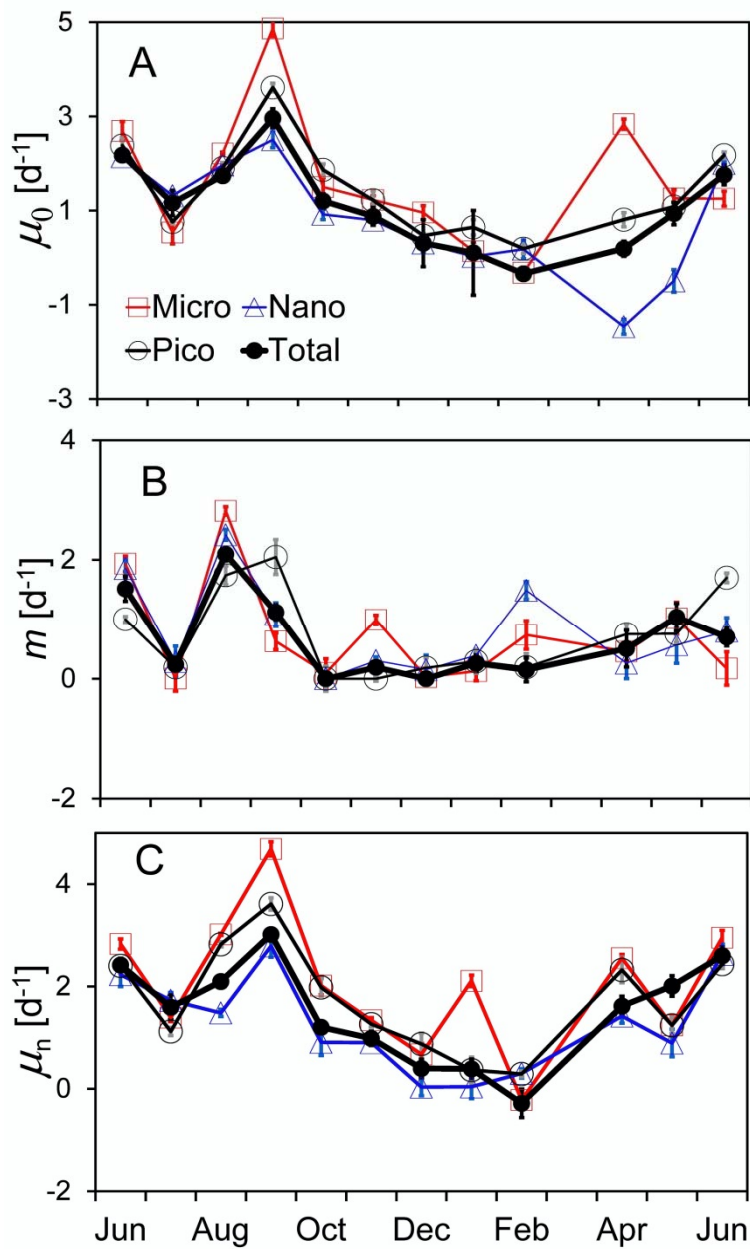
Figure 5: Temporal variations of (A) natural phytoplankton growth rate (μ_0), (B) microzooplankton grazing rate (m), and (C) nutrient enriched phytoplankton growth rate (μ_n), as well as their size-fractionated components for micro-, nano-, and pico-cells at the Wanshan station from June 2018 to June 2019. Error bars are standard errors from dilution fits.
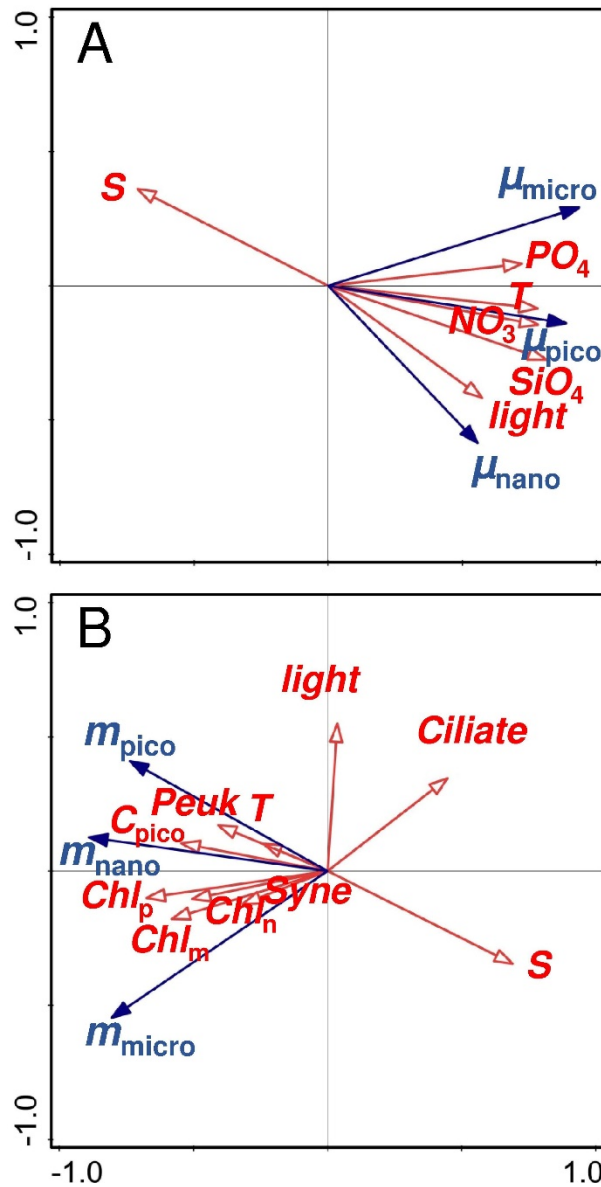
Figure 6: Redundancy analyses (RDA) representing (A) the relationships of the size-fractionated phytoplankton growth rates (μ_{micro}, μ_{nano}, and μ_{pico}) with various environmental variables and (B) the relationships of the size-fractionated microzooplankton grazing rates (m_{micro}, m_{nano}, and m_{pico}) with various environmental variables. Red arrows are environmental variables with blue arrows for rates; Chl_m, Chl_n, and Chl_p are the chlorophyll-a concentrations of micro-, nano-, and pico-phytoplankton; C_{pico} is the picophytoplankton carbon biomass with *Peuk* for the picoeukaryote and *Syne* for the *Synechococcus*.
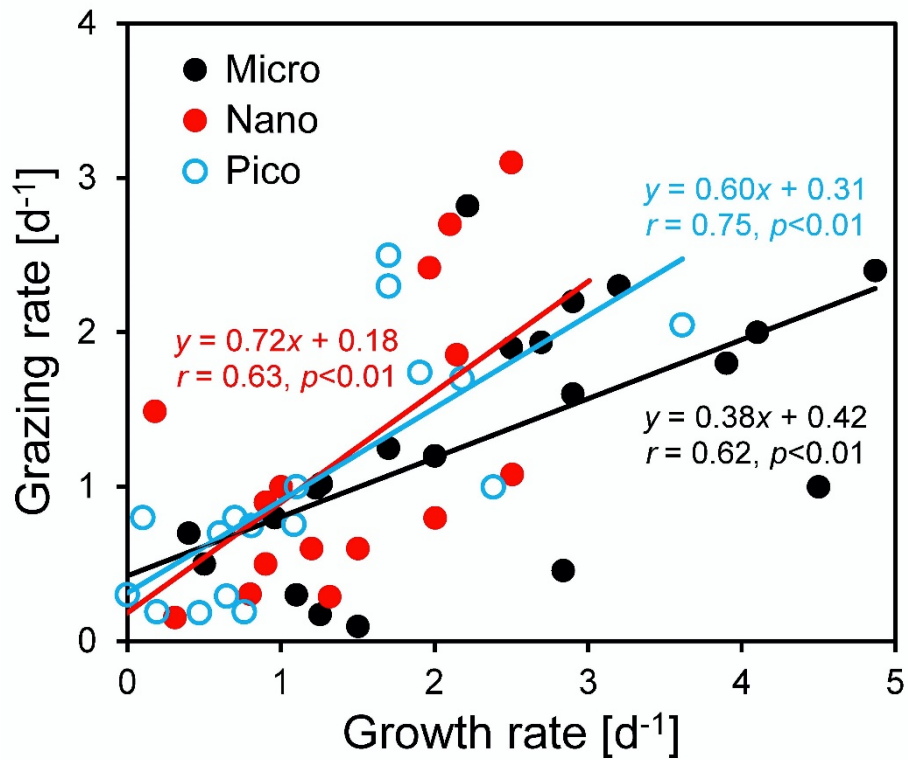
Figure 7: Regressions between natural phytoplankton growth rate and microzooplankton grazing rate for micro-, nano-, and pico-cells in the coastal northern South China Sea outside the Peral River Estuary. Note that negative rates have been excluded from the regression.

595